The structure of fluid trifluoromethane and methylfluoride

2000 J. Phys.: Condens. Matter 12 8765

(http://iopscience.iop.org/0953-8984/12/41/302)

J. Phys.: Condens. Matter **12** (2000) 8765–8776. Printed in the UK PII: S0953-8984(00)13918-9

The structure of fluid trifluoromethane and methylfluoride

J Neuefeind†, H E Fischer‡‖ and W Schröer§

† Hamburger Synchrotronstrahlungslabor HASYLAB at Deutsches Elektronensynchrotron DESY, Notkestr 85, D-22603 Hamburg, Germany
‡ Institut Laue-Langevin, 6 rue Jules Horowitz, BP 156, 38042 Grenoble Cedex 9, France
§ Inst. f. Anorg. und Phys. Chem, Univ. Bremen, Leobener Strasse NW II, D-28359 Bremen, Germany

Received 16 May 2000, in final form 25 July 2000

Abstract. We present hard x-ray and neutron diffraction measurements on the polar fluorocarbons HCF_3 and H_3CF under supercritical conditions and for a range of molecular densities spanning about a factor of ten. The Levesque–Weiss–Reatto inversion scheme has been used to deduce the site–site potentials underlying the measured partial pair distribution functions. The orientational correlations between adjacent fluorocarbon molecules—which are characterized by quite large dipole moments but no tendency to form hydrogen bonds—are small compared to a highly polar system like fluid hydrogen chloride. In fact, the orientational correlations in HCF_3 and H_3CF are found to be nearly as small as those of fluid CF_4, a fluorocarbon with no dipole moment.

(Some figures in this article are in colour only in the electronic version; see `www.iop.org`)

1. Introduction

The understanding of the dielectric properties resulting from orientational correlations [1, 2], as well as the determination of orientational correlations from diffraction experiments [3, 4], are long standing problems in the physics of molecular fluids. The simple fluorocarbons HCF_3 and H_3CF are very interesting model substances in this context, as they possess rather large dipole moments ($1.65 \times 3.336 \times 10^{-30}$ C m in the case of HCF_3—the same as that of the water molecule) but no tendency to form hydrogen bonds [5]. The investigation of the structure of the simple fluorocarbons H_3CF and HCF_3 thus enables the study of the structural effect of the molecular dipole alone.

Although the properties of these fluorocarbons are interesting, only very limited structural information is available so far. HCF_3 is considered as a replacement for chlorinated hydrocarbons as a refrigerant since it has no ozone damaging effects, it has a shorter atmospheric lifetime and hence a lower global warming potential, and it presents no toxological risk [6, 7]. HCF_3 is discussed for extraction applications [8] and it has been shown that the enatioselectivity of asymmetric catalysis can be controlled by the density of the HCF_3 solvent [9]. The crystal structure of HCF_3 has been determined by a neutron powder diffraction experiment [10] and the molecular geometry by a gas phase electron diffraction study [11]. The only fluorocarbon previously investigated in the supercritical regime is tetrafluoromethane (CF_4) [12], whereas deuterated trifluoromethane (DCF_3) has been investigated in the liquid regime [13, 14]. In both cases the total neutron structure factor was determined. References to

‖ Present address: Laboratoire pour l'Utilisation du Rayonnement Electromagnétique (LURE), Centre Universitaire Paris-Sud, BP 34, 91898 Orsay cedex, France.

0953-8984/00/418765+12$30.00

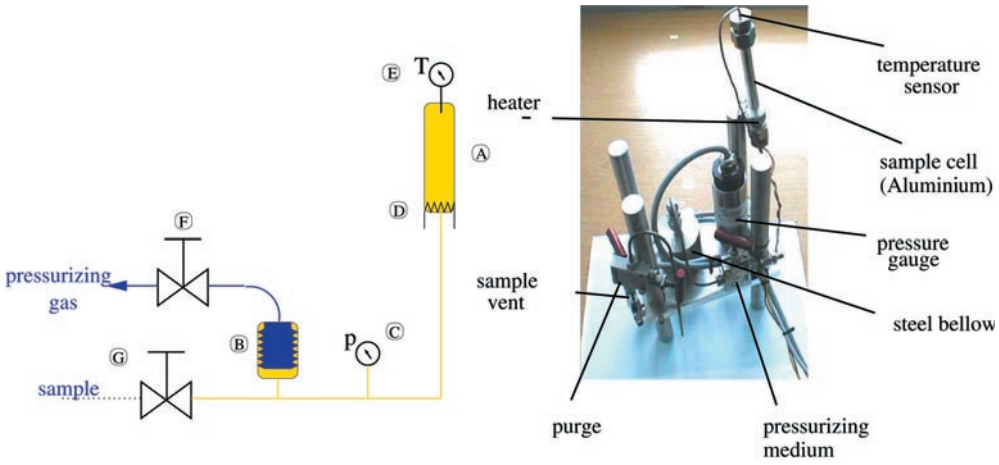

Figure 1. Schematic drawing and picture of the pressure set-up: A, sample container; B, steel bellow; C, pressure sensor; D, heater; E, temperature sensor; F, vent for the pressurizing medium; G, sample vent.

the simulation studies performed for HCF_3 can be found in the recent work by Hloucha and Deiters [15] beginning with the early work of Böhm *et al* [16].

The method used here to deduce molecular orientations is based on the potential inversion scheme of Levesque *et al* [17]. From the results of hard x-ray and neutron diffraction experiments with isotopic substitution (NDIS) a site–site potential is deduced, which in turn can be used in an NVT–Monte Carlo simulation to obtain the orientational correlations. The determination of the potential is facilitated by the ease with which the density of these systems can be varied, both having a critical point at about room temperature.

2. Experimental

We have investigated the structure of the fluid fluorocarbons in a range of pressures (28–100 bar) and temperatures (298–333 K) around the critical points of 58 bar, 317.8 K for H_3CF and 48.3 bar, 299.1 K for HCF_3 [18]. It was intended to combine the information of an NDIS experiment [19, 20] and a hard x-ray diffraction experiment [21]. The neutron and hard x-ray experiments were both carried out using the same sample environment (figure 1) built especially for this experiment. The mechanical requirements of the pressure cell are moderate, and aluminium is a very suitable material for the sample container. Aluminium has a quite low scattering power for both neutrons and x-rays, only a few powder lines due to its cubic structure and shows only a little activation in a neutron beam. The samples, DCF_3 (98% D, Cambridge isotopes), HCF_3, a 1:1 mixture HCF_3/DCF_3 and H_3CF (all Linde technical gases) can be condensed into the sample container through immersion in liquid nitrogen. The cell is then mounted inside a vacuum tank of the neutron or hard x-ray diffractometer. The sample pressure inside the mounted cell can be varied via an inert gas line, separated by a steel bellow from the sample. The temperature can be varied with a small heater at the bottom of the cell. The price of the deuterated gases requires the reduction of dead volumes inside the cell: the cell can be filled with $\sim$4 g of the sample.

The neutron diffraction measurements were performed at the diffractometer D4b [22] at the ILL reactor source in Grenoble, using a wavelength of 0.7501 Å. Representative

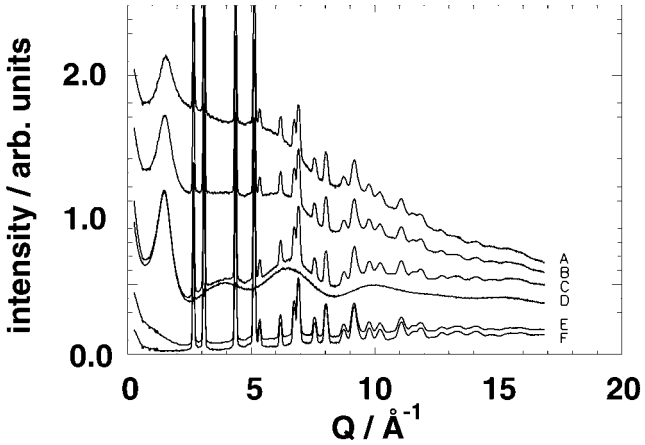

Figure 2. Raw data of the neutron diffraction experiment on trifluoromethane at D4b. A–C, sample + cell scattering intensity of HCF_3, MCF_3 (the H/D mixture) and DCF_3 respectively at liquid-like densities (30 °C, 100 bar); D, scattering intensity of C after subtraction of the cell scattering; E, sample + cell scattering intensity of DCF_3 at gas-like densities (60 °C, 32 bar); F, empty aluminium container.

examples of the raw data are shown in figure 2, showing that the aluminium cell is clearly a viable alternative to the more usual vanadium and titanium–zirconium cells. The hard x-ray diffraction was performed at the high-energy beamline BW5 at the DORIS storage ring at HASYLAB, Hamburg in its set-up for liquid and amorphous substances [23], using a wavelength of 0.1282 Å.

3. Data analysis

The data were corrected for systematic effects like detector dead time, absorption, container scattering, multiple and incoherent scattering, using the procedure described in some detail in [24], and then normalized. The differential cross sections are expressed in terms of the scattering functions $S^{(x)}(Q)$ and $S^{(n)}(Q)$ for the hard x-ray and the neutron cases

$$S^{(n)}(Q) = \frac{(\mathrm{d}\sigma/\mathrm{d}\Omega)^{(n)} - \sum_i^{N_{uc}} \nu_i b_i^2}{(\sum_i^{N_{uc}} \nu_i b_i)^2} + 1 \tag{1}$$

$$S^{(x)}(Q) = i(Q) + 1 = \frac{(\mathrm{d}\sigma/\mathrm{d}\Omega)^{(x)}/\sigma_{el} - \sum_i^{N_{uc}} \nu_i f_i^2}{(\sum_i^{N_{uc}} \nu_i f_i)^2} + 1 \tag{2}$$

where $(\mathrm{d}\sigma/\mathrm{d}\Omega)$ is the coherent differential cross section; b_i is the coherent scattering lengths [25]; f_i are the x-ray form factors in the independent atom approximation [26]; σ_{el} is the scattering cross section of the free electron; ν_i is the stoichiometric coefficient of the atom i; and where the sums are extending over the number of distinct atoms in the molecule N_{uc}, the subscript uc refers to the unit of composition, the molecule. In figure 3 the density dependence of the x-ray structure function of H_3CF is shown. Beyond $Q \sim 2.5$ Å^{-1} the interference scattering intensity is dominated by the intramolecular contributions. Fitting of the Debye equation in the range $(4 < Q < Q_{max})$

$$i(Q)_{intra} = \sum_{i \neq j} 2 \frac{f_i f_j}{(\sum_i^{N_{uc}} \nu_i f_i)^2} \frac{\sin(Q r_{ij,eq})}{Q r_{ij,eq}} \exp(-Q^2 \gamma_{ij}^2/2) \tag{3}$$

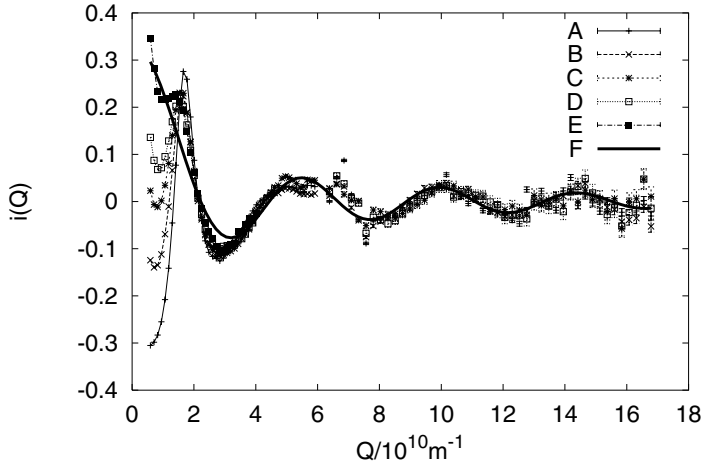

Figure 3. X-ray structure function $i(Q)$ of H_3CF at various densities. A, $\rho_{uc} = 17.6 \times 10^{-3}$ Å^{-3}; B, $\rho_{uc} = 13.0 \times 10^{-3}$ Å^{-3}; C, $\rho_{uc} = 10.4 \times 10^{-3}$ Å^{-3}; D, $\rho_{uc} = 7.3 \times 10^{-3}$ Å^{-3}; E, $\rho_{uc} = 2.6 \times 10^{-3}$ Å^{-3}; F, fit of equation (3) to the data with $r_{CF} = 1.416(8)$ Å and $\gamma_{CF} = 0.050(18)$ Å.

Table 1. Molecular structure of HCF_3. All distances and displacement parameter in Å, all angles in degrees.

	This work, fluid	Crystal [10]	Gas phase [11]
r_{CF}	1.327	1.315(4)[b]	1.3284(31)
r_{FF}	2.153		
r_{HC}	1.088	1.111(7)	1.091(14)
r_{HF}	1.995		
γ_{CF}	0.092		
γ_{FF}	0.104		
γ_{HC}	0.112		
γ_{HF}	0.145		
∠HCF	111.0[a]	109.77(32)[b]	110.35
∠FCF	108.4[a]	109.14(43)[b]	108.58(44)

[a] The angles are not refined directly, but determined from the maxima of the distance distributions.
[b] Mean value of intramolecular distances and bond angles non equivalent in the crystal.

with $r_{ij,eq}$ the equilibrium distance of the atoms i and j within the molecule and γ_{ij} the displacement parameter, leads to $r_{CF} = 1.416(8)$ Å and $\gamma_{CF} = 0.050(18)$ Å independent of density. Likewise, the molecular parameters of trifluoromethane were determined and are shown in table 1. For trifluoromethane the molecular parameters are also independent of the density and in excellent agreement with the gas phase values from [11]. For the remainder of the article only the intermolecular contributions to the structure are considered.

The intermolecular scattering contribution is related to the weighted intermolecular pair distribution functions by a Fourier-sine transformation:

$$r(g^{(n)} - 1) = \frac{1}{2\pi^2 \rho_{uc}} \int Q(S^{(n)} - 1) \sin(Qr)\, \mathrm{d}Q \tag{4}$$

$$r(g^{(x)} - 1) = \frac{1}{2\pi^2 \rho_{uc}} \int Q i(Q) \sin(Qr)\, \mathrm{d}Q. \tag{5}$$

where ρ_{uc} is the density per unit of composition (molecule). $g^{(x)}$ and $g^{(n)}$ and are weighted sums of the partial (site–site) pair distribution functions (PPDF):

$$g^{(n)} = \sum_{ij} w_{ij} g_{ij} \qquad \text{with } w_{ij} = \frac{\nu_i \nu_j b_i b_j}{(\sum_i \nu_i b_i)^2} \tag{6}$$

and

$$g^{(x)} = \sum_{ij} \mathrm{FT}[w_{ij}(Q)] \otimes g_{ij} \qquad \text{with } w_{ij}(Q) = \frac{\nu_i \nu_j f_i(Q) f_j(Q)}{(\sum \nu_i f_i)^2} \tag{7}$$

where FT( ) is the Fourier-sine transformation and $\otimes$ the convolution operation.

Trifluoromethane has six PPDF, and four independent diffraction experiments were carried out. Consequently, assuming the independence of the structure from the isotopic composition, a set of one PPDF (HH) and three independent composite partial pair distribution functions (CPPDF) can be isolated, each of the CPPDF is the weighted sum of two PPDF. The three CPPDF are dominated by the fluorine PPDF, FF, FC and FH, while the carbon PPDF, CC and HC do contribute only very little. Alternatively the total pair distribution function can be split into HH, HX and XX CPPDF, with X being either C or F. This is the same separation as that used in the case of the hydrogenhalides, with X = Cl in that case, thus enabling a proper comparison of our results with measurements of the structure of fluid HCl. All pair distribution functions are defined such that $\lim_{r\to\infty} g(r) = 1$.

4. Potential inversion

In order to generate a three-dimensional picture of the structure from the pair distribution functions, the potential inversion scheme of Levesque *et al* [17] (LWR-scheme) was applied. The idea of this method is based on the equation

$$g(r) = \exp\left(\frac{-v(r)}{kT} + g(r) - 1 - c(r) + B(r, v)\right) \tag{8}$$

relating the pair distribution function and the pair potential, where $v(r)$ is the pair potential, $c(r)$ is the direct correlation function and $B(r, v)$ the bridge function.

The direct correlation functions can be obtained by solving the site–site Ornstein–Zernike (SSOZ) equation (see e.g. [27]). The aim of liquid state theories is in general to derive the distribution functions from a potential. In this case, the structure factor and not the potential is known beforehand and hence no closure relation is needed at this point to proceed. The use of the SSOZ equation implies the knowledge of all PSF, which is not given (see the previous section). Instead the following equation, strictly valid for monoatomic liquids has been used for the determination of the direct correlation function

$$c(r) = \frac{1}{2\pi^2 \rho r} \int Q\left(1 - \frac{1}{S(Q)}\right) \sin(Qr)\, \mathrm{d}Q. \tag{9}$$

It is noted, that the SSOZ equation reduces to the multicomponent OZ equation, if the $\hat{\omega}$ matrix [27] is the identity matrix and the multicomponent OZ equation reduces to the OZ equation for monoatomic systems, if the elements of the $\hat{h}$ matrix (the PSF) are all similar, as in the present case.

From the experimental point of view, the dependence on $1/S(Q)$ is interesting to note. In dense liquids of low compressibility, $S(Q)$ is small at low momentum transfers and the direct correlation function is especially sensitive to these regions (cf the case of liquid gallium in [28]). Whether an extrapolation of the measured $S(Q)$ to low momentum transfers is necessary depends on the maximum distance r_{max} at which $c(r)$ is structured. For r_{max} = 15 Å

a minimum momentum transfer of $\pi/r_{max} \sim 0.2$ Å^{-1} is sufficient. In the present case where the density is low and compressibility is high $S(Q)$ is not as small at low momentum transfers and the above limitations are not important.

Starting with a first guess of the potential $v^{(1)}$, e.g. by neglecting the bridge function, a Monte Carlo simulation gives $g(r)^{(1)}$ and $c(r)^{(1)}$ belonging to $v^{(1)}$ and thus $B(r, v^{(1)})$. Substituting $B(r, v^{(n-1)})$ for $B(r, v)$ in equation (8) gives the LWR iteration formula

$$v^{(n)}/kT = v^{(n-1)}/kT + \ln(g^{(n-1)}/g^{(exp)}) + c^{(n-1)} - c^{(exp)} - g^{(n-1)} + g^{(exp)}. \tag{10}$$

Schommers [29] proposed a similar iteration scheme where only the logarithmic term of equation (10) is considered. Reatto *et al* [30] have shown that their algorithm converges—under certain conditions much faster than the Schommers scheme. Soper's EPMC algorithm [31] uses the same iteration scheme as Schommers, except that it is formulated for multi-element fluids. Likewise, it has been shown by Kahl and Kristufek [32] that the LWR scheme is applicable to polyatomic systems. The systems investigated here are even a step more complicated than the systems Kahl and Kristufek used, as the sites are connected by covalent bonds and the PPDF are not complete. Thus the HC and the CC site–site potentials were kept constant as hard sphere potentials. The method has already been tested under these conditions and compared to the results of reverse Monte Carlo (RMC) [33] simulations. A short account of the comparison between the potential inversion and the RMC method has been given elsewhere [34]. In the following only the results of the potential inversion method are given.

The potential determined from the LWR-scheme is an effective two-body potential and accounts for many-body effects implicitly. Unlike a true two-body potential, an effective two-body potential thus may be state dependent [35]. Figure 4 demonstrates the correct prediction of the pair distribution function at several different state points from a pair potential determined at a specific state point.

5. Simulation details

The Monte Carlo simulations were performed in the NVT ensemble. All simulations were performed with 297 flexible five-site molecules in a cube with the conventional periodic boundary conditions. The half-box length varies with density from 16.2 Å to 35.4 Å. The iterative inversion has been done at $\rho_{uc} = 1.15 \times 10^{-3}$ Å^{-3} corresponding to a half-box length of 31.8 Å. No corrections for long-range forces are possible as nothing is known about the inverted potential beyond these 31.8 Å (this problem is also discussed in [30]). The simulation box is fairly large, however, so that the potential is effectively zero at half-box length. If the molecular radius is taken to be the CF bond length plus the *van der Waals radius* of the fluorine atom, the half-box length at $\rho_{uc} = 1.15 \times 10^{-3}$Å^{-3} is twelve times the molecular radius. A single MC move of a molecule consists of a translation and a rotation of the molecular frame. Additionally, the individual atoms were moved relative to their equilibrium position in the molecular frame, so that the experimental intramolecular Debye–Waller factors (see above) are reproduced. The configurations were equilibrated for 10^5 accepted moves and the simulation was then run for further 3×10^5 accepted moves to calculate the averages.

In principle, the LWR scheme can be started from an arbitrary starting potential. Two starting potentials have been chosen, one by neglecting the bridge function as described above and one from an exp-6-type potential [36]. After about ten LWR iteration cycles the potential is converged in the sense, that further application of the RLW scheme does not decrease the agreement with experiment. The iteration has been run for a total of 23 LWR iterations. The final potential used for the further simulations is the average of iterations 6 to 23.

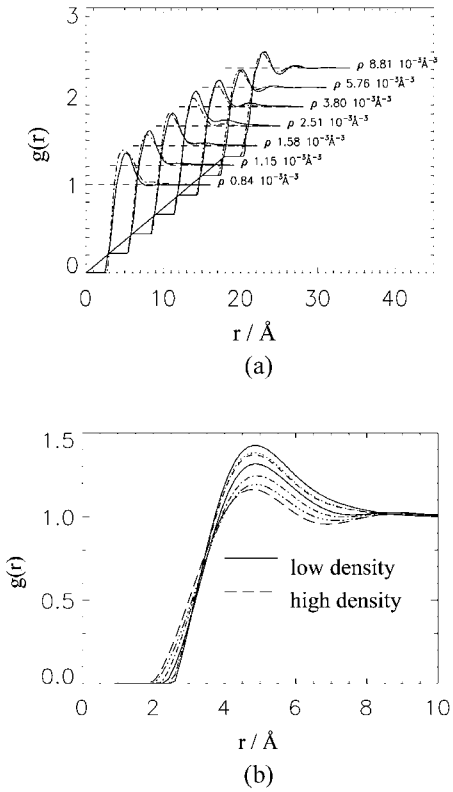

Figure 4. (a) Example of the density dependence of the intermolecular part of the $g_{XX}^{(n)}$ CPPDF of HCF_3. The experimental $g_{XX}^{(n)}$ (dashed line) is compared with the prediction of a potential model (full line) derived at some specific state point (f: $\rho_{uc} = 1.15 \times 10^{-3}$ Å^{-3}). The results for subsequent state points are shifted by +3 units in the x-direction and +0.22 units in the y-direction. (b) Direct comparison of the experimental $g_{XX}^{(n)}$ at decreasing density (same state points as in (a)). The densities in the figure correspond to the pressures and temperatures given in table 2.

Table 2. Experimental conditions of the diffraction experiments on trifluoromethane

	Pressure/bar	Temperature/K	Density10^{-3}Å^{-3}
a	100	298	8.8
b	100	333	5.8
c	80	333	3.8
d	60	333	2.5
e	50	333	1.6
f	40	333	1.15
g	32	333	0.84

6. Results and discussion

In figure 4(a) the density dependence on $g_{XX}^{(n)}$ of trifluoromethane is shown. The density dependence of the other CPPDF is similar. At the higher densities $g_{XX}^{(n)}$ shows a typical liquid-like behaviour and several maxima and minima. The maxima at larger distances die out when lowering the density, while the height of the first maximum increases. This is contrary to the

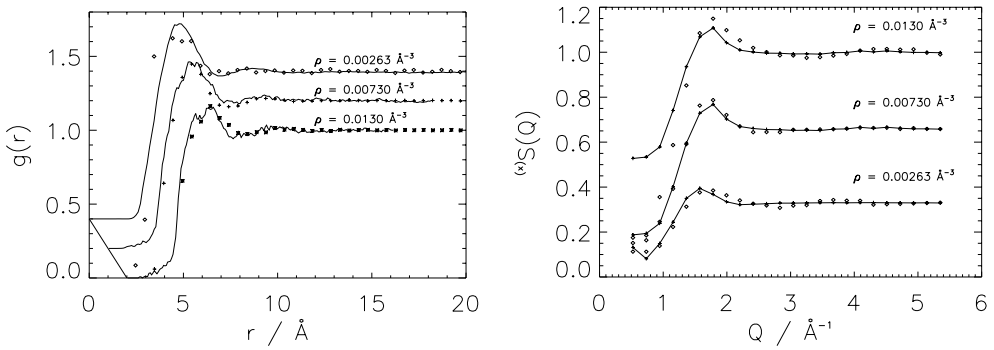

Figure 5. Comparison of (a) $g^{(x)}(r)$ and (b) ${}^{(x)}S(Q)$ for H_3CF from the experiment with the result from a Monte Carlo simulation using the site–site potentials derived for HCF_3. (a) The symbols correspond to the experimental $g^{(x)}(r)$, the separation of the symbols in the x-direction corresponds to the experimental resolution, the full curve to the simulation. The $g^{(x)}(r)$ correspond to different densities shown in the figure (state point B, D and E in figure 3). The results for subsequent state points are shifted by 1.0 units in the x- and +2.0 units in the y-direction for clarity. (b) Crosses joined with a full curve belong to the simulation, diamonds to the experiment. The results for subsequent state points are shifted by 0.33 units in the y-direction.

behaviour of fluid hydrogen chloride [38] or water [39] where the height of the main maximum decreases with density. The position of the main maximum remains almost unchanged.

The HCF_3 molecular potential has been determined as a site–site potential, whereas for H_3CF only the x-ray weighted pair distribution function $g(r)^{(x)}$ was determined, and thus an independent determination of H_3CF site–site potentials was not possible. The question arises as to whether the HCF_3 site–site potentials can also be used to describe the H_3CF structure, i.e. if these potentials have a general applicability to all fluorocarbons. Figure 5 indicates that the site–site potentials are indeed transferable to a different molecular species. It is, however, noted that at the largest density, the simulated $S(Q)$ does not extrapolate to the correct $Q \to 0$ limit and the peak position is shifted.

The aim of the present work was to determine the influence of the molecular dipole on the orientational correlations between the molecules. Figure 6 compares the HH, HX and XX pair distribution functions of fluid HCl [38], HCF_3 and H_3CF. The three PPDF of HCl are quite structured and dissimilar while the corresponding CPPDF of both HCF_3 and H_3CF are much less structured and are very similar. This behaviour is an indication that there will be no strong preference for particular orientations in the fluorocarbons. The most remarkable difference can be seen in the XX-(C)PPDF: g_{ClCl} in HCl has the highest maximum.

Figure 7 quantifies this qualitative statement and shows $P(r_{COM}, \cos(\theta))$, the relative probability of finding a second molecule at the centre of mass distance r_{COM} in an orientation $\cos(\theta)$, where θ is the angle between the molecular dipoles. This figure is to be compared to figures 5 and 7 of [38] and to figure 9 of [12]. While the first work determines the orientational correlation in fluid HCl via the EPMC formalism (truncated version of (10)) and finds pronounced orientational correlations, the second is a RMC study using a total neutron structure factor measurement of fluid CF_4 as input and finds a $P(r_{COM}, \theta)$ very similar to figure 7, structured only at very short distances.

Averaging the mean $\langle\cos(\theta)\rangle$ via

$$g_K = 1 + \int_0^\infty N(r)\langle\cos(\theta)\rangle_r \, \mathrm{d}r \tag{11}$$

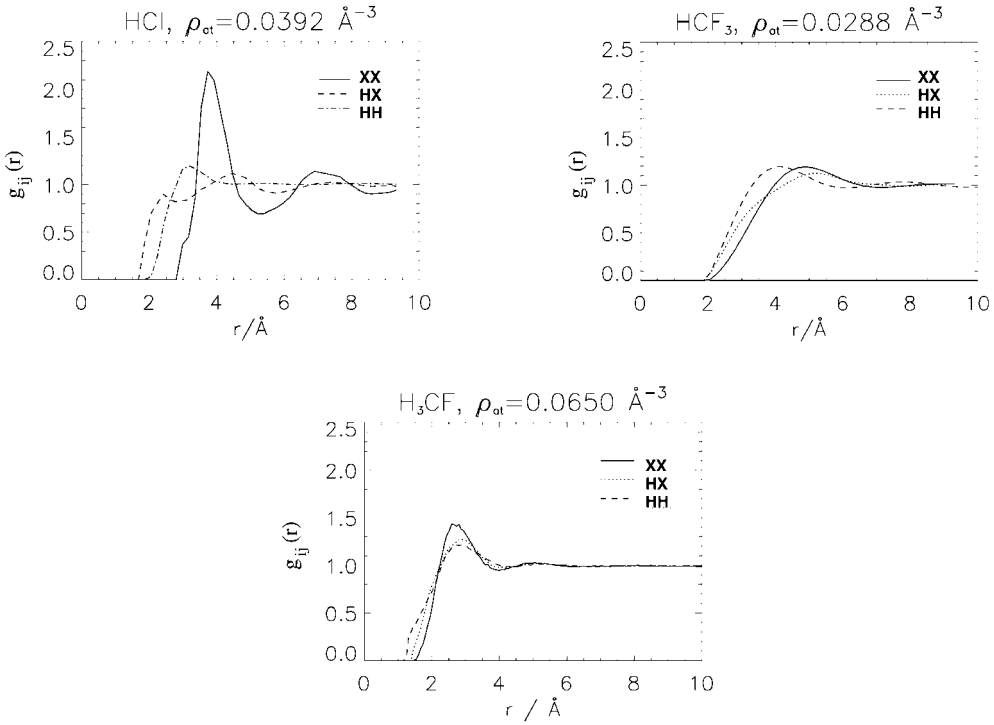

Figure 6. Comparison of the HH, HX and XX CPPDF of HCF_3 and H_3CF with the PPDF of HCl [38]. The CPPDF for H_3CF are simulation results.

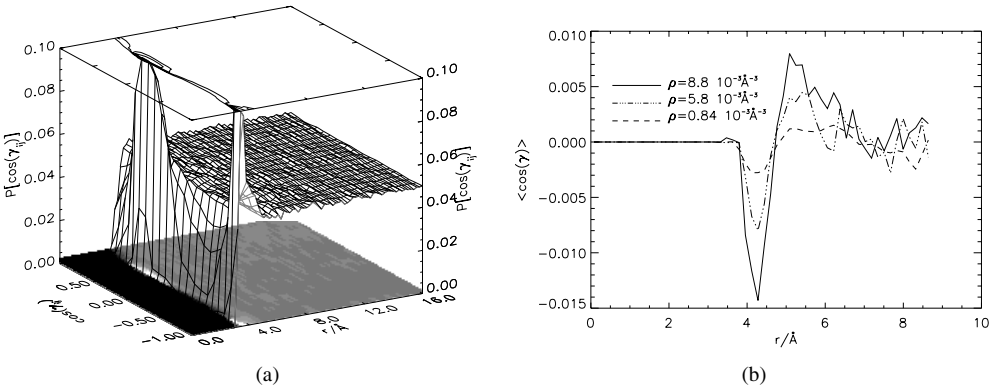

Figure 7. (a) Cosine distribution of the angle θ between the molecular dipoles of HCF_3 at $\rho = 8.8$ 10^{-3} Å^{-3}; (b), mean cosine of the angle θ *versus* the centre of mass distance at three different densities.

with $N(r) = 4\pi\rho_{uc}r^2 g_{COM}$, to yield a Kirkwood g-factor leads to values very close to one (0.995 on average) in the entire density range investigated for both HCF_3 and H_3CF. This is in agreement with advanced theories of the dielectric properties of these materials [37].

The largely simplified model illustrated in figure 8(a) can help to understand this behaviour. At a distance of 5 Å, the maximum of the pair distribution functions of HCF_3, the energy difference between parallel and antiparallel alignment of point dipoles of

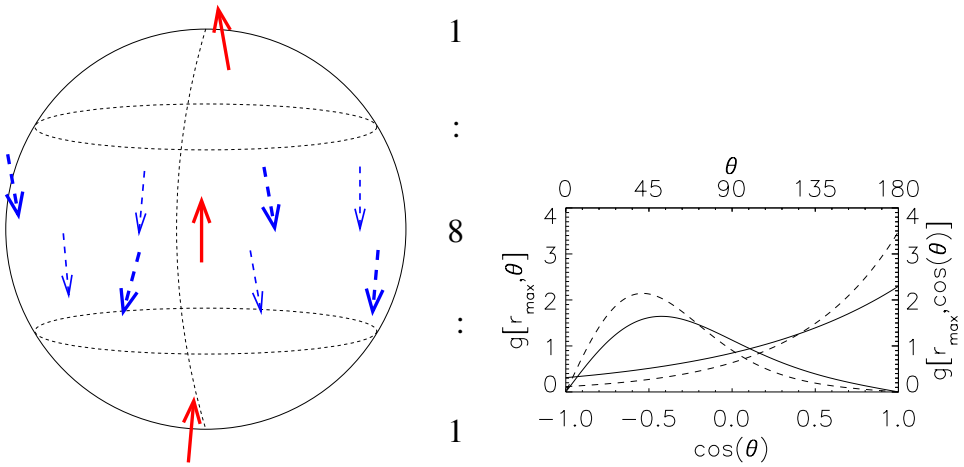

(a) (b)

Figure 8. (a) Simplified model of the relative orientation of dipolar molecules. Explanation in the text. (b) Cosine distribution and theta distribution to be expected from two point dipoles in polar arrangement for $p = 1.65 \times 3.336 \times 10^{-30}$ C m, $r_{max} = 5$ Å (HCF_3, full curve) and $p = 1.07 \times 3.336 \times 10^{-30}$ C m, $r_{max} = 3.6$ Å (HCl, broken curve).

$1.65 \times 3.336 \times 10^{-30}$ C m located at the centre of mass is about $2\,kT$ for the polar positions and about $1\,kT$ for the equatorial positions. In a two-level system this would lead to seven times more parallel than antiparallel orientations at the two polar positions and three times more antiparallel orientations at the equatorial positions. But the equatorial region is four times larger, leading to an almost complete cancellation of parallel and antiparallel orientations.

For HCl a preference for a polar arrangement of molecules has been found [38] (molecules directly 'below' or 'on top' of each other referred to the direction of the dipole). For these molecules in polar arrangement a strong preference for parallel orientations has been found—up to 17 times more parallel orientated dipoles than expected from a random distribution. The cosine distribution to be expected for point dipoles in a polar arrangement is

$$P[r, \cos(\theta)] = \frac{\exp[k(r)\cos(\theta)]}{\int_{-1}^{1} \exp[k(r)\cos(\theta)]\,\mathrm{d}\cos\theta} \tag{12}$$

with $k(r) = 2p^2/4\pi\epsilon r^3$. This function is shown for $r = r_{max}$, with r_{max} the first maximum of $g(r_{COM})$ in figure 8(b). With $p = 1.07 \times 3.336 \times 10^{-30}$ C m [40] and $r_{max} = 3.6$ Å (HCI) thus only 3.5 times more parallel oriented dipoles as in a random distribution should be found. From a simple point dipole model a less pronounced preference of parallel orientation as found by [38] is predicted for HCl, while on the other hand from this model a stronger preference than actually found would be expected for both HCF_3 and H_3CF, probably due to the detailed molecular geometry and specific site–site interactions. These two effects, the cancellation of parallel and anti-parallel orientations and specific site–site interactions lead finally to the average behaviour shown in figure 7 very similar to fluid CF_4.

Hloucha and Deiters [15] recently published a constant NPT–Monte Carlo simulation of liquid HCF_3 at subcritical temperatures. Their model uses a rigid 5-site structure, with a Lennard-Jones contribution to the potential, partial charges at the sites and point dipoles at the centre of mass, with a constant and an induced contribution. With this model and in the dense liquid they find more pronounced orientational correlations between neighbouring molecules than we do. The positive peak in $\langle\cos(\theta)\rangle_r$ at $r \sim 4.5$ Å in figure 7 is higher by a

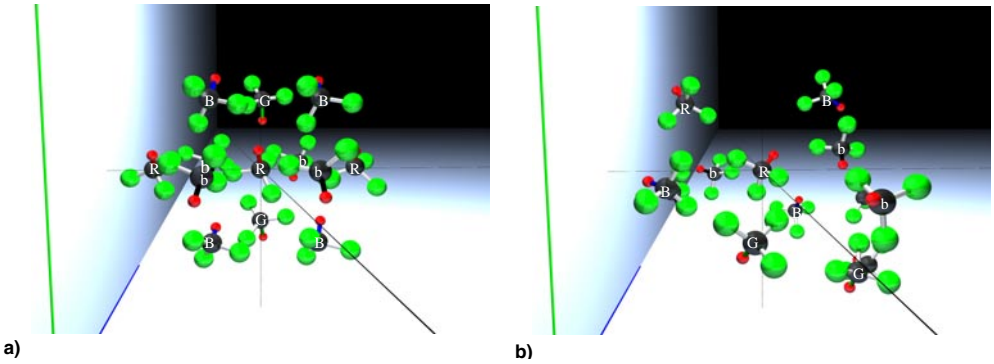

Figure 9. Relative orientation of next-neighbour molecules in (a) crystalline HCF_3 and (b) dense fluid HCF_3. The relative orientation to the central molecule is indicated with a colour code. In the crystal: Red (R): parallel, green (G) antiparallel, blue (B) and black (b): different T-configurations. In the fluid: red $1.0 > \cos(\theta) > 0.5$, blue $0.5 > \cos(\theta) > 0$, green $0 > \cos(\theta) > -0.5$, black $-0.5 > \cos(\theta) > -1.0$.

factor of two and the negative peak at close contact is missing. Hloucha and Deiters observed a decreasing trend in the orientational order with decreasing density which will tend to level out the differences in orientational order in the range of densities investigated here. So the detailed comparison is complicated by the difference in the range of thermodynamic parameters investigated, but nevertheless supports the point of view that the orientational ordering in HCF_3 is even less pronounced than predicted by a dipolar picture.

The spatial arrangement of neighbouring molecules is illustrated in figure 9 which compares the crystal (a)—the positional parameters are taken from [10]—and (b) the fluid at liquid-like densities. In the crystal each trifluoromethane molecule is surrounded by twelve neighbouring molecules at nearly the same distance. Among these, two are oriented parallel and two antiparallel, the remaining two times four molecules in two different T-orientations, that are orientations where the dipole moments are perpendicular to each other. Figure 9(b) is a snap-shot of a simulation at $\rho_{uc} = 0.0088$ Å^{-3}. Again, the twelve next-neighbours are shown. The orientation of these molecules has been grouped into four classes having a $\cos(\theta)$ between -1.0 and -0.5, -0.5 and 0.0, 0.0 and 0.5 and 0.5 and 1.0, respectively, with θ the angle between the molecular dipoles. Again, quasi T-orientations occur more often. In the fluid this snap-shot is only representative of course, the ensemble of structures leads to figure 7.

7. Conclusion

NDIS and hard x-ray diffraction data of trifluoromethane (HCF_3) and hard x-ray diffraction data of fluoromethane (H_3CF) are presented here. These have been used to study the density dependence of the orientational correlations in these substances by NVT–Monte Carlo simulations using effective site–site two-body potentials derived via the Levesque–Weis–Reatto inversion scheme from the NDIS and hard x-ray diffraction data of HCF_3. Advanced theories of the dielectric properties of these materials predict a Kirkwood g-factor close to one in the entire density range investigated here. The orientational correlations found in the simulation are in full agreement with this prediction. A detailed comparison with the orientational correlations found in fluid hydrogenchloride (HCl) and tetrafluoromethane (CF_4) shows that the orientational correlation in HCF_3 and H_3CF are closer to CF_4 than to HCl, although the interaction energy of the molecular dipoles is comparable to HCl in these systems.

This and the comparison with the simulation results for a dipolar model of HCF_3 suggests that in the fluorocarbons a site specific interaction results in weaker orientational correlations than predicted by a dipolar model while in fluid HCl the orientational ordering is enhanced, presumably due in part to stronger H-bonding effects.

Acknowledgments

The assistance of P Palleau and O Koch during the neutron experiment and the help of A Swiderski in constructing the pressure cell is gratefully acknowledged.

References

[1] Buckingham A D 1967 *Adv. Chem. Phys.* **12** 107
[2] Schröer W 1985 *Adv. Chem. Phys.* **63** 719
[3] Zeidler M D 1982 *Z. Phys. Chem.* **133** 1
[4] Soper A K, Andreani C and Nardone M 1994 *Phys. Rev.* E **47** 2598
[5] Reuter K, Rosenzweig S and Franck E U 1989 *Physica* A **156** 294
[6] Pires P F and Guedes H J R 1999 *J. Chem. Thermodynam.* **31** 479
[7] Fermeglia M and Pricl S 1999 *Fluid Phase Equil.* **166** 21
[8] Zhao J and Olesik S V 1999 *Fluid Phase Equil.* **154** 261
[9] Wynne D C and Jessop Ph G 1999 *Angew. Chem. Int. Ed.* **38** 1143
[10] Torrie B H, Binbrek O S and Powell B M 1996 *Molec. Phys.* **87** 1007
[11] Kawashina Y and Cox A P 1978 *J. Molec. Spectrosc.* **72** 423
[12] Waldner I, Bassen A, Bertagnolli H, Tödheide K, Strauss G and Soper A K 1997 *J. Chem. Phys.* **107** 10 667
[13] Mort K A, Johnson K A, Cooper D L, Burgess A N and Howells W S 1997 *Molec. Phys.* **90** 415
[14] Hall C D, Johnson K A, Burgess A N, Winterton N and Howells W S 1991 *Molec. Phys.* **74** 27
[15] Hloucha M and Deiters U K 1998 *Fluid Phase Equil.* **149** 41
[16] Böhm H J, Meissner C and Ahlrichs C J 1984 *Molec. Phys.* **53** 651
[17] Levesque D, Weis J J and Reatto L 1985 *Phys. Rev. Lett.* **54** 451
[18] Lide D R (ed) 1998 *CRC Handbook of Chemistry and Physics* (Boca Raton, FL: Chemical Rubber Company)
[19] Enderby J E, North D M and Egelstaff P A 1966 *Phil. Mag.* **14** 961
[20] Suck J B, Raoux D, Chieux P and Riekel C (eds) 1992 *Methods in the Determination of Partial Structure Factors of Disordered Matter by Neutron and Anomalous X-Ray Diffraction* (Singapore: World Scientific)
[21] Poulsen H F, Neuefeind J, Neumann H-B, Schneider J R and Zeidler M D 1995 *J. Non-Cryst. Sol.* **188** 63
[22] Ibel K (ed) 1994 *Guide to Neutron Research Facilities at the ILL* (Grenoble: ILL)
[23] Bouchard R, Hupfeld D, Lippmann T, Neuefeind J, Neumann H-B, Poulsen H F, Rütt U, Schneider J R, Süssenbach J and v. Zimmermann M 1998 *J. Synchrotron Rad.* **5** 90
[24] Weitkamp T, Neuefeind J, Fischer H E and Zeidler M D 2000 *Molec. Phys.* **98** 125
[25] Köster L, Rauch H and Seymann E 1991 *At. Data Nucl. Data Tab.* **49** 65
[26] Hubell J H, Veigele W J, Briggs E A, Brown R T, Cromer D T and Howerton R J 1995 *J. Phys. Chem. Ref. Data* **4** 471
[27] Enciso E 1987 *Molec. Phys.* **60** 617
[28] Bellissent-Funel M-C, Chieux P, Levesque D and Weis J J 1989 *Phys. Rev.* A **39** 6310
[29] Schommers W 1983 *Phys. Rev.* A **28** 3599
[30] Reatto L, Levesque D and Weis J J 1986 *Phys. Rev.* A **33** 3451
[31] Soper A K 1996 *Chem. Phys.* **202** 295
[32] Kahl G and Kristufek K 1994 *Phys. Rev.* E **49** 3565
[33] McGreevy R L and Pusztai L 1988 *Mol. Sim.* **1** 359
[34] Neuefeind J, Fischer H E and Schröer W 2000 *Physica* B **276–278** 481
[35] Allen M P and Tildesley D J 1989 *Computer Simulation of Liquids* 2nd edn (Oxford: Clarendon)
[36] Gavezotti A 1982 *Nouv. J. Chim.* **6** 443
[37] Schröer W, Labrenz D, Rybarsch C and Dorfmüller Th (eds) 1989 *Reactive and Flexible Molecules in Liquids* (Deventer: Kluwer) p 141
[38] Andreani C, Ricci M A, Nardone M, Ricci F P and Soper A K 1997 *J. Chem. Phys.* **107** 214
[39] Soper A K, Bruni F and Ricci M A 1997 *J. Chem. Phys.* **106** 247
[40] Greenwood N N and Earnshaw A 1984 *Chemistry of the Elements* (Oxford: Pergamon)